Nuclear Engineering and Technology 54 (2022) 834–841

Contents lists available at ScienceDirect

Nuclear Engineering and Technology

journal homepage: www.elsevier.com/locate/net

Original article

Application of artificial neural network for the critical flow prediction of discharge nozzle

Hong Xu [a, *], Tao Tang [a, b], Baorui Zhang [c], Yuechan Liu [d]

[a] Energy Technology R&D Division, Jinyuyun Energy Technology Co., Ltd., Chongqing, China
[b] School of Microelectronics and Communication Engineering, Chongqing University, Chongqing, China
[c] Institute of Nuclear and New Energy Technology, Tsinghua University, Beijing, China
[d] Department of Mathematics, Karlsruhe Institute of Technology (KIT), Germany

ARTICLE INFO

Article history:
Received 22 May 2021
Received in revised form
15 July 2021
Accepted 25 August 2021
Available online 13 September 2021

Keywords:
Two-phase critical flow
Nuclear safety
Genetic neural network (GNN)
Artificial neural network (ANN)
Genetic algorithm (GA)
Critical pressure ratio

ABSTRACT

System thermal-hydraulic (STH) code is adopted for nuclear safety analysis. The critical flow model (CFM) is significant for the accuracy of STH simulation. To overcome the defects of current CFMs (low precision or long calculation time), a CFM based on a genetic neural network (GNN) has been developed in this work. To build a powerful model, besides the critical mass flux, the critical pressure and critical quality were also considered in this model, which was seldom considered before. Comparing with the traditional homogeneous equilibrium model (HEM) and the Moody model, the GNN model can predict the critical mass flux with a higher accuracy (approximately 80% of results are within the ±20% error limit); comparing with the Leung model and the Shannak model for critical pressure prediction, the GNN model achieved the best results (more than 80% prediction results within the ±20% error limit). For the critical quality, similar precision is achieved. The GNN-based CFM in this work is meaningful for the STH code CFM development.

1. Introduction

Nuclear safety is the most significant concern for nuclear power plants (NPPs). Various measures need to be taken to ensure that all related equipment and facilities are in normal operation or safe shutdown reducing the possibility of NPP accidents. It is required that certain corresponding safety measures should be implemented based on the emergency procedures when accidents (e.g., the most common loss-of-coolant accidents (LOCAs) or steam generator tube ruptures (SGTRs)) occur. Based on the NPP design criteria, the design basic accident (DBA) scenarios are analyzed in detail to obtain the NPP operating license [1]. Consequently, system thermal-hydraulic (STH) codes, such as RELAP5, ATHLET, CATHARE and MARS, etc. [2], were developed and widely used for the analysis. The accuracy of the STH codes is heavily dependent on their thermal-hydraulic models [3].

According to the sensitivity study [4], the critical flow (also called choked flow), which is caused by the leakage of two-phase coolant from the high-pressure primary side of the NPP loop and is limited by the sound speed of the two-phase flow condition [5], may impact the accuracy of STH with a relatively higher sensitivity during the transient simulation of the accident scenario. Actually, in order to achieve high accuracy of STH codes, the critical flow model was focused on in the nuclear community from the 1950s until now [6,7], with a variety of critical flow models developed. The traditional critical flow models can be divided into three types: simplified analytic models, fitted functions and numerical models based on the conservation equations [8]. Since the first two models are less accurate compared with the third one, the trend in the last two decades was to develop the non-homogeneous non-equilibrium models for the two-phase critical flow [9,10], considering both the velocity and the temperature differences between the two phases during the choking process, and achieving the critical mass flow rate by solving a 6- or 7- ordinary differential equations (ODEs) based on the two-phase mass, momentum and energy conservation equations. These models are more accurate but one disadvantage of these models is that it is time-consuming to achieve the critical mass flow rate since the system of ODEs is normally stiff or ill-conditioned around the critical point. It is not suitable to use in the STH code directly [11]. To overcome these difficulties of the traditional critical flow models, artificial neural networks (ANNs),

* Corresponding author.
E-mail address: xuhong2005@tsinghua.org.cn (H. Xu).

https://doi.org/10.1016/j.net.2021.08.038

which can achieve a higher accurate and more efficient model, are resorted to in this paper.

Actually, ANNs have been used widely in nuclear engineering since the 1990s, which have been summarized in the review work of Cong et al. [12] and Gomez-Fernandez et al. [13] with totally hundreds of references. But if one focuses on the critical flow models based on the machine learning methods, there were very limited researches in the literature and, furthermore, the majority of the researches were concentrated on the refrigerant fluid, e.g., R12, R134a, and R407C, etc. [14–16]. For example, A.A. Aly et al., have used ANN to predict the critical mass flux of R22 and R407C (totally 200 datasets) [17]. It was seldom to use water as the fluid to develop the machine-learning-based critical flow models. Obviously, it is valuable for nuclear engineering, especially for the critical flow research of light water reactors (LWRs). Zhang et al. [18] have used two kinds of ANNs to build the critical flow model for the mass flow prediction of Leak Before Break (LBB) under a variety of conditions. Consequently, their models were suitable to the leakage prediction for the cracks, with an accuracy of 22.7% (relative error), which was better than the existing correlations at that time. An et al. [19] have developed an ANN-based critical flow model by using the data obtained from the existed model (Henry-Fauske) to predict the critical mass flux of break at saturated or subcooled conditions. Following the work of An et al., Park et al. [20] have used the ANN-based critical flow model in the LOCA simulation of an optimized power reactor-1000. Although they achieved a very high accuracy compared with the prediction results of the Henry-Fauske model and the simulation results of the MAAP code, its prediction accuracy needs to be evaluated based on the experimental data.

Based on the background above, this work plans to develop an ANN-based critical flow model based on the Sozzi-Sutherland tests [21]. This work used the genetic neural network (GNN), which is a sophisticated approach and has been widely concerned and used. Therefore, the algorithm is not the focus of this work. The characteristics and main contributions of this work can be summarized as follows:

1. Use the experimental data with a wider scope of upstream conditions to develop the GNN-based critical flow model. In order to avoid the impact of human operations on the data and model, all experimental data of the test database was used for the training and verification of the network model.
2. While the literature only concentrated on the critical mass flux prediction, this paper developed more detailed models for some other parameters (i.e., the pressure and the quality of the fluid at the choking point) of the critical flow. In this way, the developed ANN-based critical flow model will be more powerful and applicable in the STH codes.

The rest of this paper is organized as follows. Section 2 will introduce the Sozzi-Sutherland database firstly and then the detailed GNN procedure. Section 3 will discuss the GNN optimization process and show the predicted results of the GNN model (comparing with other typical models). The conclusion of the work is presented in Section 4.

2. GNN methodology

In order to overcome the drawback to conventional ANN (slow convergence and may converge to the local optimal solution, weak generalization ability, etc.) and to achieve higher efficiency, intelligent optimization algorithms (e.g., Genetic Algorithm (GA), Particle Swarm Optimization (PSO), etc.) were often adopted to optimize the conventional ANN structure or parameters. The most commonly used method is the genetic neural network (GNN), which could be thought of as a combination of GA and conventional ANNs. It has the advantages of both conventional ANNs and GA [22]. GNN has been used widely in the field of engineering, and nuclear engineering is no exception with several applications. Consequently, there is no plan to describe the methodology of GNN again, only highlight some key points. For details of the GNN, some literature may be resorted to Refs. [23,24]. As a background, the Sozzi-Sutherland database will be introduced firstly in this section, and then the detailed GNN procedure will be illustrated step by step.

2.1. Databases

Sozzi-Sutherland tests were classical data sources for the critical flow model development [25,26]. Each Sozzi-Sutherland critical flow test was conducted by discharging high-pressure water from a vessel to the atmosphere. Several types of pressure vessels and flow path geometries were designed. In this work, all the test data (229 tests totally) from two types of nozzles are selected for the critical flow prediction based on GNN. In the tests, the critical mass flux measurements have been made with saturated and sub-cooled water. This parameter is dependent on pressure, fluid enthalpy, flow path geometry, size and length. The parameter ranges of the selected Sozzi-Sutherland critical flow database are listed in Table 1.

This work also concentrates on the critical pressure and critical quality at the choking point, which have been seldom studied by the ANN method before. In the Sozzi-Sutherland tests, the distribution of the critical pressure ratio, which is defined as the ratio of the critical pressure at the choking point to the upstream stagnation pressure, is shown in Fig. 1. For one-dimensional ideal isentropic flow, there is a theoretical solution for the ratio, which is a function of the specific heat ratio (C_P/C_V) and has a value of approximately 0.5 [27]. But for the real fluid, especially the two-phase flow, this ratio depends on the fluid upstream thermodynamic condition (e.g., the stagnation pressure, temperature, quality, etc.) and the geometry of the discharge flow path (e.g., the shape of the discharge flow path, the inner diameter, the length, etc.) [28]. These complex factors lead to the dispersed distribution in Fig. 1.

2.2. GNN procedure

In this work, the widely used back propagation (BP) algorithm is chosen for training feed-forward ANN. But due to the defects of the BP algorithm, GA is used for the optimization of BP-ANN weights and biases. The weights and biases of BP-ANN are transformed into the chromosome of GA. The flowchart for the overall critical mass flux prediction procedure by GNN is shown in Fig. 2, which is divided into three parts: (1) build BP-ANN network; (2) GA part; (3) BP-ANN part (to optimize the weights and biases further and to predict the critical flow parameters).

2.2.1. Build BP-ANN network

BP-ANN is adopted to build the critical flow model in this work. The 4 parameters in Table 1 are chosen as the inputs of the network. As a result, the GNN-based critical flow model can be represented

Table 1
Parameter ranges of the Sozzi-Sutherland critical flow databases.

Parameter	Minimum	Maximum
Discharge pipe L/D ratio/-	0.37	3.50
Upstream pressure/MPa	3.03	7.07
Subcooling/°C	0	69.46
Equilibrium quality	−0.006	0.007

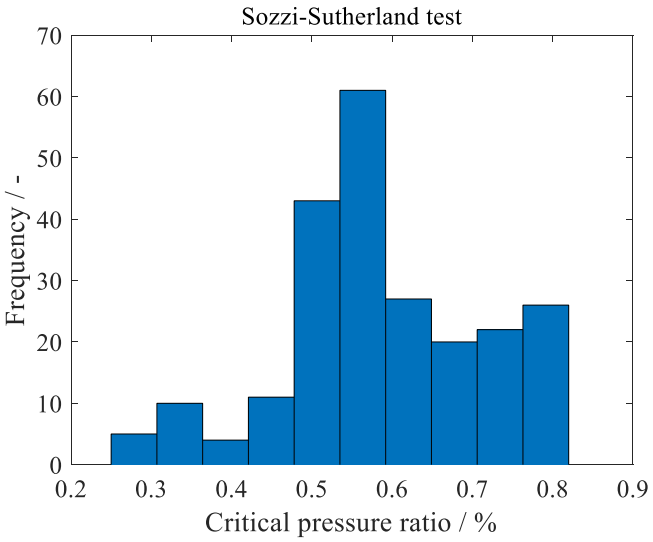

Fig. 1. Critical pressure ratio in the Sozzi-Sutherland test.

as Eq. (1).

$$G_{cr} = f(L/D,\ P, T,\ x) \tag{1}$$

It should be emphasized that the pressure and quality at the choking point are predicted by the network, which have never been considered in the literature related to machine learning methods in this field before. The neuron number of the hidden layer needs to be selected based on the network performance, which will be studied in section 3.2. As a typical BP-ANN, we assume that the hidden layer is set to have 5 neurons here. Therefore, the BP-ANN structure is $4 \times 5 \times 3$, as shown in Fig. 3. In order to make the network training more effective, its input and output parameters are normalized before the training step. After the prediction values are achieved, they need to be denormalized correspondingly.

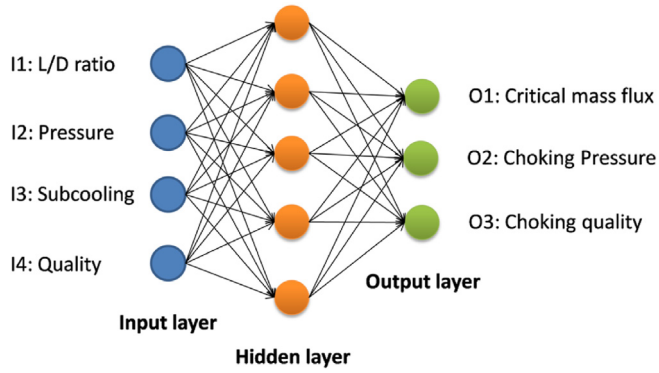

Fig. 3. Schematic sketch of the BP-ANN structure.

The tan-sigmoid function (i.e., "tansig") is used as the transfer function for the input layer. As shown in Eq. (2), regarding any input n, it can transfer the output between −1 and 1.

$$tansig(n) = \frac{2}{1+e^{-2n}} - 1 \tag{2}$$

A linear transfer function (i.e., "purelin") is used in the hidden layer. For the output layer, the Levenberg–Marquardt algorithm (i.e., "trainlm") is used.

2.2.2. GA part

The weights and biases of BP-ANN are represented by chromosomes in the GA. There are normally three methods for chromosome coding: symbol coding, binary coding and floating-point coding. For the GA optimization, it can be divided into the following steps:

- Step 1: create an initial random population (initialize weights and biases). Set the evolution generation counter $g = 0$ and the

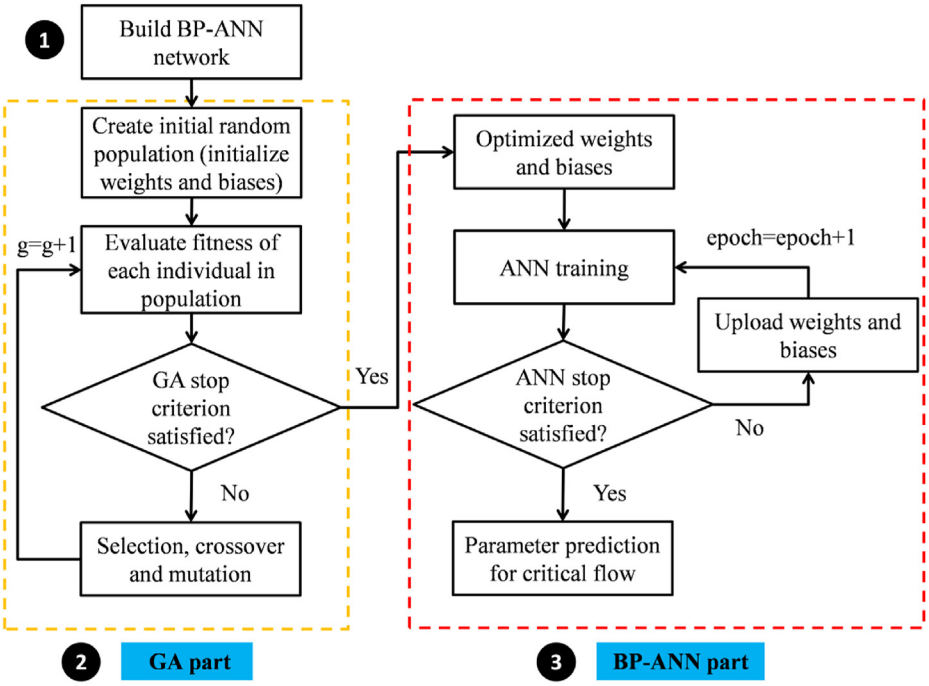

Fig. 2. The overall critical mass flux prediction procedure by GNN based on experimental databases.

largest evolution generation G. Subsequently, M individuals are randomly generated as the initial population $P(0)$;

- Step 2: evaluate the fitness of each individual in the population. The fitness of each individual in population $P(g)$was calculated and evaluated. The fitness function and its value are used for the evaluation of the performance of each individual. In this work, the fitness function is defined as reciprocal of the error squaring sum between prediction values and goal values. The low fitness individuals will be deleted and only the chromosomes, which have high fitness values, are reserved. Based on the fitness function, it is assumed that the calculated fitness value of each chromosome is $F_i, (i = 1, 2, \cdots M)$, then the selection probability p_i of each chromosome is Eq. (3).

$$p_i = F_i \Big/ \sum_{i=1}^{M} F_i, (i = 1, 2, \cdots M) \tag{3}$$

- Step 3: crossover and mutation. The operation of crossover is used to generate new individuals for the population, to explore the solution space. The crossover operation of chromosome a_k and chromosome a_l at the location j is Eq. (4) (w is a random number related to the crossover probability).

$$a_{kj} = w \cdot a_{kj} + (1 - w) \cdot a_{lj}, a_{lj} = (1 - w) \cdot a_{kj} + w \cdot a_{lj}, \tag{4}$$

The mutation is an operator of GA, which keeps the diversity of the population. The mutation of chromosome a_{ij} is shown in Eq. (5)

$$a_{ij} = \begin{cases} a_{ij} + (a_{max} - a_{ij}) \cdot r_2 \cdot (1 - g/G)^2, \ when\ r > 0.5 \\ a_{ij} + (a_{ij} - a_{min}) \cdot r_2 \cdot (1 - g/G)^2, \ when\ r \leq 0.5 \end{cases} \tag{5}$$

a_{max} and a_{min} are the upper and lower of chromosome a_{ij}, respectively. r and r_2 are random numbers. g and G are the generation counter and the largest evolution generation.

- Step 4: based on the genetic operation (selection, crossover, mutation) of the population $P(g)$, a new generation of population $P(g+1)$ will be obtained.
- Step 5: termination criterion satisfied? The termination criterion is that the largest evolution generation G is achieved.

Since the adopted BP-ANN structure is $4 \times 5 \times 3$, there are total of 43 parameters for the weights and bias of BP-ANN. They are transformed into the chromosome of GA with the length 43. In the whole operation process of GA, the selection of parameter settings has a great impact on the results. So far, there is no systematical perfect theory to guide how to set the appropriate parameters. The main parameters include coding length, population size, fitness function, crossover probability, mutation probability and iteration times. These parameters can affect the optimization efficiency and calculation accuracy of GA [29]. In this study, the following GA parameters were set for the GA optimization. The maximum generation, population size, crossover probability and mutation probability are 500, 30, 0.2 and 0.1, respectively.

2.2.3. BP-ANN part

Since the network has been built in part 1 of the GNN procedure in Fig. 2, this part is only the execution of ANN iteration to optimize the ANN weights and biases further and to predict the key parameters of the critical flow. The parameters were set as shown in Table 2. The maximum number of epochs to training was 100. The learning rate affects the convergence speed and performance of the network. The higher the learning rate, the faster the learning speed, but the performance of the network will be reduced. In this study, the learning rate was 0.1. The performance goal was used to end training and was set at 0.00001. The Sozzi-Sutherland critical flow databases were divided randomly into two parts: 70% as training data and the other as test data. The training data was used for the training of BP-ANN to optimize the parameters and the test data for an independent test of the prediction capability of the trained ANN. The iteration was terminated if the criteria (the maximum epoch or the performance goal was achieved) were satisfied. After the iteration of training was finished, the test database was used for the critical flow parameter prediction.

Table 2
Setting of BP-ANN parameters.

Parameter	Value
maximum number of epochs for training	100
learning rate	0.1
performance goal	0.00001
training ratio	0.7
testing ratio	0.3

3. Results and discussion

The GNN optimization will be discussed firstly and then, the results of three typical critical flow parameters (critical mass flux, critical pressure and critical quality) will be shown and compared with other models, respectively.

3.1. GNN optimization process

The fitness values reflect the performance of GA during the evolution epochs. Its main trend is shown in Fig. 4. The fitness values went up very sharply at the first 150 generations and after that, the values increased slowly and went to convergence at last.

3.2. Evaluation of model for parameter prediction

In order to evaluate the effectiveness of the critical flow model based on GNN, two typical indices were introduced in this work to analyze the results of the model. These indices are the mean absolute error (MAE) and the normalized root mean square error (NRMSE), as shown in Eq. (6) and Eq. (7), respectively. The parameter G_E represents the measured value in the test and G_P

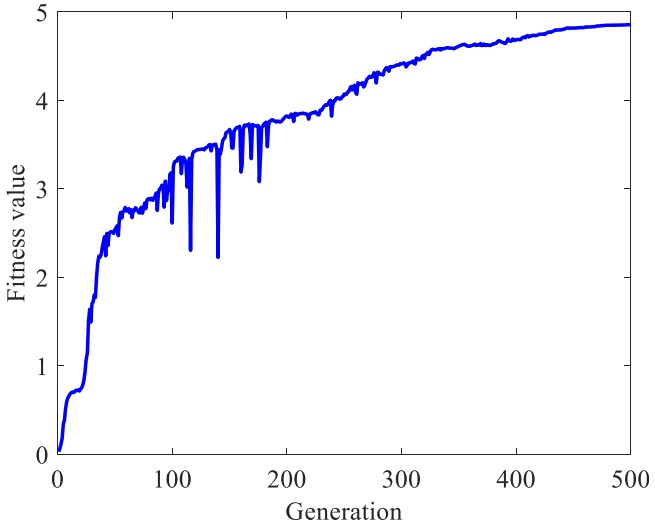

Fig. 4. Variation of fitness value with the evolution generation.

represents the prediction value by GNN. The parameter N depends on the concerning range of summation, e.g., the training database, the test database and the overall database.

$$MAE = \frac{1}{N}\sum_{i=1}^{N}\left|\frac{G_{P,i} - G_{E,i}}{G_{E,i}}\right| \tag{6}$$

$$NRMSE = \sqrt{\frac{1}{N}\sum_{i=1}^{N}\left(G_{P,i} - G_{E,i}\right)^2} \Big/ \frac{1}{N}\sum_{i=1}^{N} G_{E,i} \tag{7}$$

As described in section 2.2, the neuron number of the hidden layer needs to be selected based on the network performance. It is assumed that the neuron number may be 3 to 7. Fig. 5 shows the MAE and RMSE results of these different ANN structures for the prediction of critical mass flux. According to Fig. 5, the neuron number of the hidden layer may impact the network performance, but the differences are not so large. The best ANN structure is the ANN with a hidden layer, which has 5 neurons. Its MAEs and RMSEs for training, test, and overall performance are the smallest of all. Furthermore, both the three MAEs and the three RMSEs are nearly the same (around 0.11 and 0.15, respectively), which means the network is not over-fitting during the training.

3.2.1. Critical mass flux

Fig. 6 shows the comparison of GNN calculated and measured critical mass flux (training database and test database, separately). The dashed blue line is the ±20% error limit. According to Fig. 6, no matter the training data and the test data, the deviations between the GNN calculated critical mass flux and the measured data mostly fall into the ±20% error limit.

In order to show the accuracy of the GNN results, the traditional homogeneous equilibrium model (HEM) and Moody model [30], which are widely used in the STH codes (ATHLET and RETRAN-3D, etc. [31]), are introduced for comparison. Fig. 7 shows the comparison of the relative error distribution for critical mass flux. The results of different models are drawn in different histograms. The GNN calculated/predicted results are nearly distributed symmetrically and most of them are within small errors. The predicted results of HEM model are normally smaller than the measured

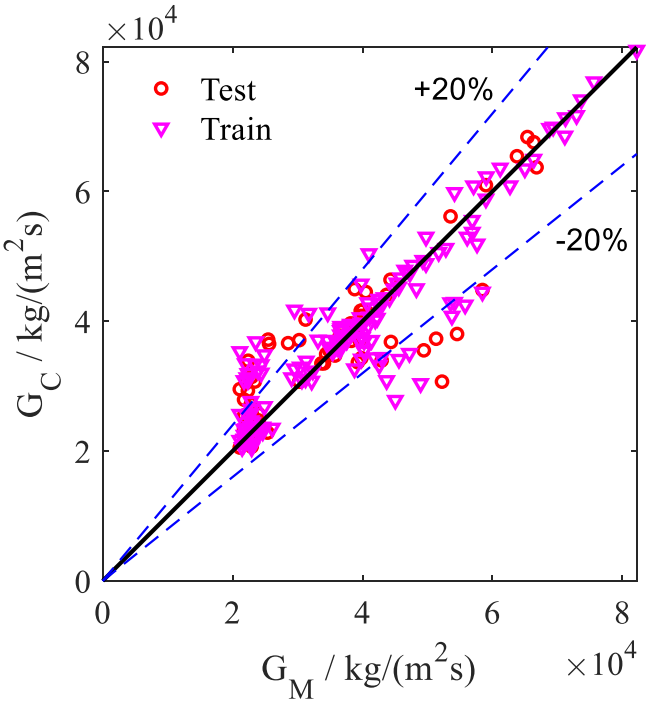

Fig. 6. Comparison of GNN calculated and measured critical mass flux.

results because it mixed the two-phase fluid as one single phase without mass transfer and heat transfer between the two phases. The conclusion of HEM under-predicted results is consistent with the literature. Moody model does not show the characteristic of under-prediction or over-prediction, but its accuracy is lower than the proposed GNN model in this study.

3.2.2. Critical pressure at choking point (choking pressure)

Fig. 8 shows the prediction results of critical pressure. The dashed blue lines are the ±20% error limit. It is obvious that most of the results calculated by the GPP model are within the ±20% error limit for both the training databases and the test databases. Since

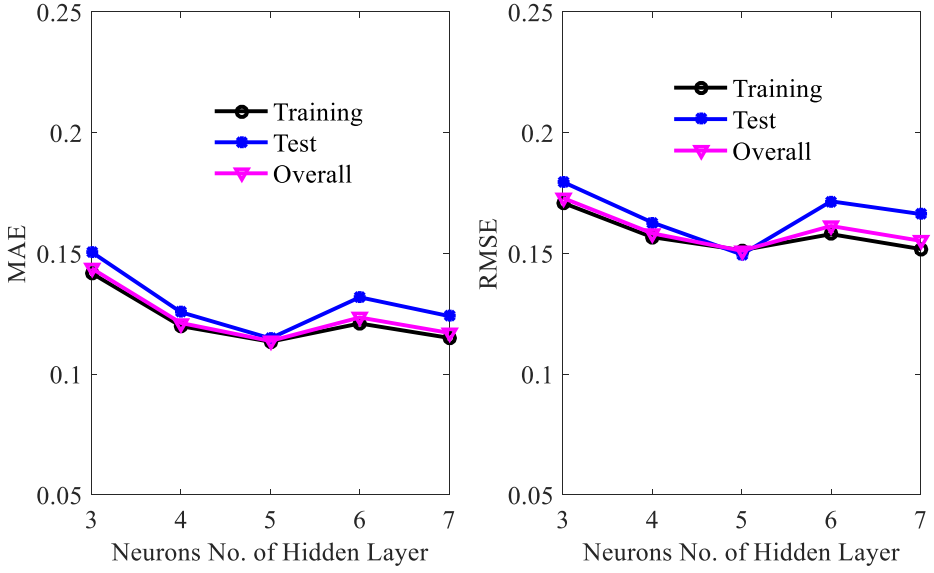

Fig. 5. Impact of hidden layer neurons number on MAE and RMSE.

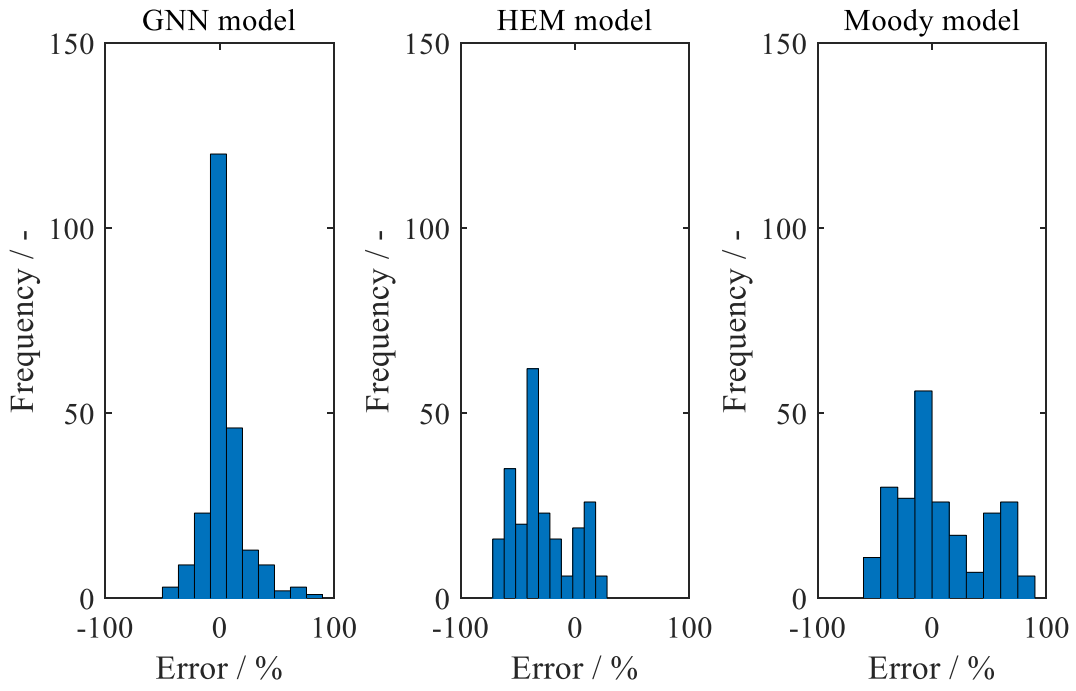

Fig. 7. Comparison of the relative error distribution for critical mass flux (the GNN model, HEM model and Moody model, respectively).

the critical pressure is a significant parameter and a focus of the critical flow model, several theoretical or empirical relations were developed for its prediction. For example, Leung [32] has developed a generalized correlation for the critical flow based on a one-component homogeneous equilibrium model (HEM), which assumed that the critical flow (including the critical pressure) was only related to the upstream condition without considering the impact of flow path geometry; Shannak [33] has built a simplified empirical correlation (against the influencing parameters, i.e. the flow path geometry and the fluid specific heat ratio) for the critical pressure ratio based on experimental data. Based on the Sozzi-Sutherland critical flow databases, a comparison of the GNN model in this work with these two typical models (legend as "Leung model" and "Shannak model") has been shown in Fig. 9. While the

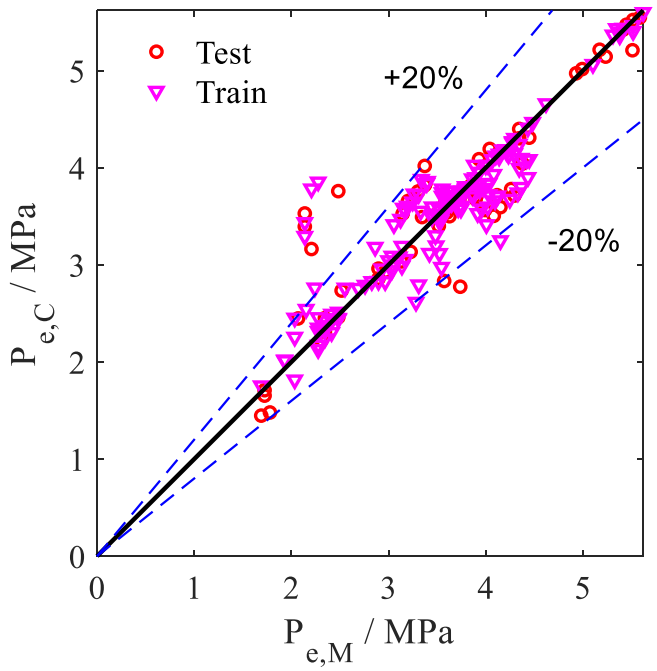

Fig. 8. Comparison of GNN calculated and measured choking pressure.

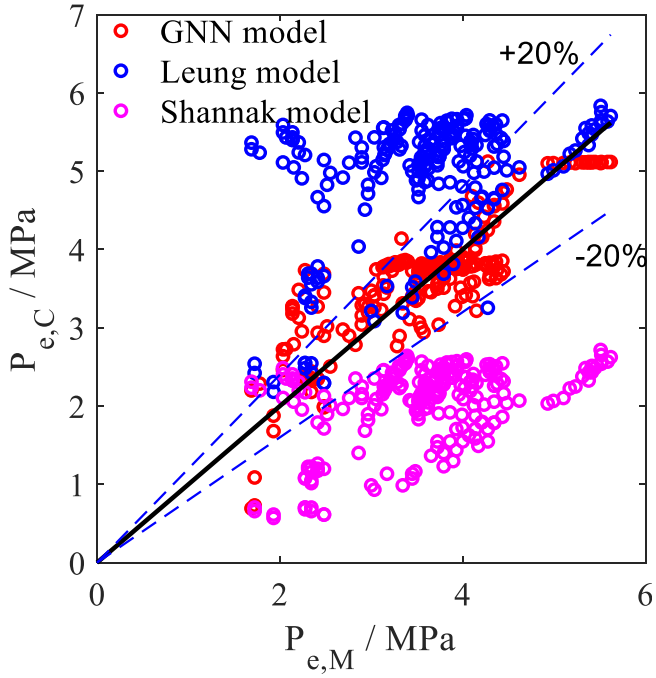

Fig. 9. Comparison of different critical pressure models.

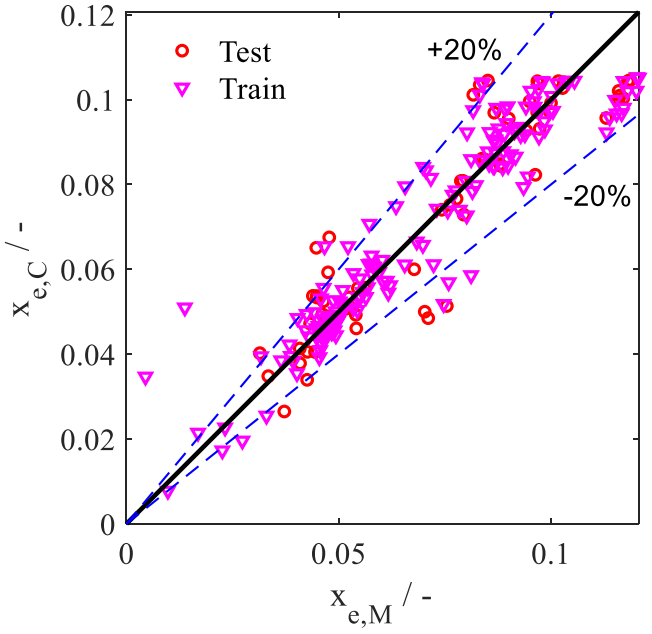

Fig. 10. Comparison of GNN calculated and measured choking quality.

Table 3
Relative error distribution for critical flow parameters.

Range / Parameter	[-20% 20%]	[-30% 30%]	[-60% 60%]	[-80% 80%]
G_C	78.3%	89.1%	99.0%	100%
$P_{e,C}$	91.7%	95.5%	99.5%	100%
$X_{e,C}$	83.8%	93.8%	99.6%	100%

Leung model over-predicts the critical pressures (not too surprising since it is based on HEM) and the Shannak model under-predict the critical pressures, the GNN model gets better results.

3.2.3. *Critical quality at choking point*

Owing to the lack of models for the critical quality in the literature, this work only gives the GNN model results, as shown in Fig. 10 for the Sozzi-Sutherland critical flow databases. Similar to the results of the critical mass flux and the critical pressure, most of the results are within the ±20% error limit.

As a summary, Table 3 gives the relative error distribution for the three critical flow parameters. For the critical mass flux and critical quality, approximately 80% results are within the ±20% error limit, 90% within the ±30% error limit. For the critical pressure, approximately 90% results are within the ±20% error limit, 95% within the ±30% error limit.

4. Conclusions

A GNN-based critical flow model has been developed in this work. To build a powerful model, besides the critical mass flux, the critical pressure and critical quality were also considered in this model, which was seldom considered before. Comparing with the HEM model and the Moody model, the GNN model in this work can predict the critical mass flux with a higher accuracy (approximately 80% results are within the ±20% error limit); comparing with the Leung model and the Shannak model for critical pressure prediction, the GNN model achieved the best results (more than 80% prediction results within the ±20% error limit). For the critical quality, similar precision is achieved.

Declaration of competing interest

The authors declare that they have no known competing financial interests or personal relationships that could have appeared to influence the work reported in this paper.

References

[1] L. Yang, Z. Chen, W. Chen, Analysis of flow path blockage accident in cased assembly, Ann. Nucl. Energy 45 (2012) 8–13.
[2] M. Hofer, M. Buck, J. Starflinger, ATHLET extensions for the simulation of supercritical carbon dioxide driven power cycles, Kerntechnik 84 (5) (2019) 390–396.
[3] H. Xu, A.F. Badea, X. Cheng, Optimization of the nodalization of nuclear system thermal-hydraulic code applied on PKL benchmark, J. Nucl. Eng. Radiat. Sci. 147 (2021) 107732.
[4] H. Xu, A.F. Badea, X. Cheng, Sensitivity analysis of thermal-hydraulic models based on FFTBM-MSM two-layer method for PKL IBLOCA experiment, Ann. Nucl. Energy 147 (2020) 107732.
[5] H. Xu, A.F. Badea, X. Cheng, Studies on the criterion for choking process in two-phase flow, Prog. Nucl. Energy 133 (2021) 103640.
[6] H.S. Isbin, J.E. Moy, A.J.R. Da Cruz, Two-phase, steam-water critical flow, Am. Ins. Chem. Eng. J. 3 (3) (1957) 361–365.
[7] R.E. Henry, H.K. Fauske, S.T. McComas, Two phase critical flow at low qualities Part I: experimental, Nucl. Sci. Eng. 41 (1) (1970) 79–91.
[8] E. Elias, G.S. Lelluche, Two-phase critical flow, Int. J. Multiphas. Flow 20 (Suppl) (1994) 91–168.
[9] S. Yin, N. Wang, X. Huang, Q. Wang, H. Wang, Characteristic of vapor leakage behavior from a pressurized pipeline system: experiment and model study, Int. J. Heat Mass Tran. 162 (2020) 120335.
[10] H. Xu, A.F. Badea, X. Cheng, Analysis of two phase critical flow with a non-equilibrium model, Nucl. Eng. Des. 372 (2021) 110998.
[11] H. Xu, A.F. Badea, X. Cheng, Development of a new full-range critical flow model based on non-homogeneous non-equilibrium model, Ann. Nucl. Energy 158 (2021) 108286.
[12] T. Cong, G. Su, S. Qiu, W. Tian, Applications of ANNs in flow and heat transfer problems in nuclear engineering: a review work, Prog. Nucl. Energy 62 (2013) 54–71.
[13] M. Gomez-Fernandez, K. Higley, A. Tokuhiro, K. Welter, W.K. Wong, H. Yang, Status of research and development of learning-based approaches in nuclear science and engineering: a review, Nucl. Eng. Des. 359 (2020) 110479.
[14] R.A. Azim, Prediction of multiphase flow rate for artificially flowing wells using rigorous artificial neural network technique, Flow Meas. Instrum. 76 (2020) 101835.
[15] C.L. Zhang, Generalized correlation of refrigerant mass flow rate through adiabatic capillary tubes using artificial neural network, Int. J. Refrig. 28 (4) (2005) 506–514.
[16] C.L. Zhang, L.X. Zhao, Model-based neural network correlation for refrigerant mass flow rates through adiabatic capillary tubes, Int. J. Refrig. 30 (4) (2007) 690–698.
[17] A.A. Aly, B. Saleh, A.M. Aljuaid, A.F. Alogla, M.M. Alharthi, Y.S. Hamed, Mass flow rate assessment in capillary tubes of refrigeration cycle powered by solar energy using back propagation artificial neural network, Int. J. Eng. Res. Technol. 12 (7) (2019) 965–976.
[18] J. Zhang, R.H. Chen, M.J. Wang, W.X. Tian, G.H. Su, S.Z. Qiu, Prediction of LBB leakage for various conditions by genetic neural network and genetic algorithms, Nucl. Eng. Des. 325 (2017) 33–43.
[19] Y.J. An, K.H. Yoo, M.G. Na, Y.S. Kim, Critical flow prediction using simplified cascade fuzzy neural networks, Ann. Nucl. Energy 136 (2020) 107047.
[20] J.H. Park, Y.J. An, K.H. Yoo, M.G. Na, Leak flow prediction during loss of coolant accidents using deep fuzzy neural networks, Nuclear Eng. Technol. 53 (8) (2021) 2547–2555.
[21] G.L. Sozzi, W.A. Sutherland, Critical Flow of Saturated and Subcooled Water at High Pressure, General Electric Co., 1975, pp. 1–24. NEDO-13418.
[22] S. Ghoshray, More efficient genetic algorithm for solving optimization problems, in: Proceedings of the IEEE International Conference on Systems, Man and Cybernetics vol. 5, 1995, pp. 4515–4520.
[23] F.H.F. Leung, H.K. Lam, S.H. Ling, P.K.S. Tam, Tuning of the structure and parameters of a neural network using an improved genetic algorithm, IEEE Trans. Neural Network. 14 (1) (2003) 79–88.
[24] S. Ding, C. Su, J. Yu, An optimizing BP neural network algorithm based on genetic algorithm, Artif. Intell. Rev. 36 (2011) 153–162.
[25] H.J. Richter, Separated two-phase flow model: application to critical two-phase flow, Int. J. Multiphas. Flow 9 (1983) 511–530.
[26] C.F. Schwellnus, M. Shoukri, A two-fluid model for non-equilibrium two-phase critical discharge, Can. J. Chem. Eng. 69 (1991) 188–197.
[27] H.S. Hillbrath, W.P. Dill, W.A. Wacker, The choking pressure ratio of a critical flow venturi, J. Eng. Ind. 97 (4) (1975) 1251–1256.
[28] F. Hardekopf, D. Mewes, Critical pressure ratio of two-phase flows, J. Loss Prev. Process. Ind. 1 (3) (1989) 134–140.

[29] G. Rudolph, Convergence analysis of canonical genetic algorithms, IEEE Trans. Neural Network. 5 (1) (1994) 96–101.
[30] F.J. Moody, Maximum two-phase vessel blowdown from pipes, Trans. ASME J. Trans. 88 (1966) 285–293.
[31] H. Xu, Improvement of PWR (LOCA) Safety Analysis Based on PKL Experimental Data, Karlsruhe Institute of Technology, Dissertation, Karlsruhe, Germany, 2020.
[32] J.C. Leung, A generalized correlation for one-component homogeneous equilibrium flashing choked flow, AIChE J. 32 (10) (1986) 1743–1746.
[33] B.A. Shannak, Experimental investigation of critical pressure ratio in orifices, Exp. Fluid 33 (2002) 508–511.